Ferromagnetic Resonance in Nickel Ferrite

W. A. YAGER, J. K. GALT, F. R. MERRITT, AND E. A. WOOD
Bell Telephone Laboratories, Murray Hill, New Jersey

(Received July 21, 1950)

The ferromagnetic resonance phenomenon in single crystals of NiO Fe_2O_3 has been studied at room temperature at 24,000 Mc/sec. Small samples were used in order to avoid electromagnetic cavity-type resonances. The g-factor observed is 2.19. The first-order magnetocrystalline anisotropy constant K_1 was found to be -6.27×10^4 ergs/cc. The absorption line was very narrow (half-widths less than 100 oersteds) and fit a resonance curve quite satisfactorily.

I. INTRODUCTION

FERROMAGNETIC resonance, originally discovered by Griffiths[1] and explained phenomonologically by Kittel,[2] has now been discussed by several authors.[3] The phenomenon has been studied in ferrites in the form of ceramics by Hewitt[4] and by Beljers[5] and in the form of single crystals of Fe_3O_4 by Bickford.[6]

We have studied the resonance behavior of single crystals of NiO Fe_2O_3 with a view to examining some of the fundamental properties of ferrites. The investigation was carried out at a frequency of approximately 24,000 Mc/sec. on spherical samples. In order to avoid electromagnetic cavity type resonances in our samples we have found it necessary to use spheres whose diameter was less than 0.1 cm. Most of our data were taken on spheres of diameter about 0.038 cm.

We have examined the field at resonance and the line width as a function of crystallographic orientation. From the first of these we find the magnetocrystalline anisotropy. The growth of the crystals and measurements of several of their properties are described elsewhere.[7]

II. EXPERIMENTAL

A block diagram of the r-f equipment used for the measurements is shown in Fig. 1. The signal oscillator is monitored with a crystal detector so that its output can be held constant. This output passes through an attenuator and then through the test cavity in which our sample is mounted. This signal is then mixed with the signal from a beat oscillator and the difference frequency passes through an attenuator, is amplified in the i-f amplifier, then detected and applied to the vertical plates of an oscilloscope. Since the beat oscillator is swept at 60 cycles over a frequency band larger than the two megacycle band width of the i-f amplifier, and since the same 60-cycle signal is used for the horizontal oscilloscope sweep the detected signal is just the shape of the i-f response curve. The peak height on the oscilloscope can be adjusted by means of the i-f attenuator, and when this height is held at a constant level the attenuator reading is a measure of the signal amplitude transmitted through the test cavity.[7a] The procedure for deriving the characteristics of the sample from signals measured in this way is given below.

A detailed picture of the test cavity showing how the sample is mounted is given in Fig. 2. By rotating the phosphor-bronze rod while the sample is in place, data can be taken at various orientations of crystal axes with respect to the r-f and steady magnetic fields.

The spherical shape of the samples was achieved using a device developed for the purpose by Bond.[8] We have produced spheres with diameters from 0.02 to 0.10 cm with the device without difficulty.

The sample is mounted on a rod as shown in Fig. 2, with its crystal axes oriented in a predetermined way. In order to do this, the crystal is first adjusted to the desired orientation by means of x-ray techniques while it is mounted on an adjustable head and can therefore be rotated by measured angles. It is attached to this head with rochelle salt which is melted and then allowed to solidify around the sample. When the head adjustments have been made, and the desired crystal axis is parallel to the axis of the head, the sample is transferred to the rod. This is done outside the cavity, and the rod is put in place in the cavity later. The head and the rod are placed in aligned V-blocks so that the ends of both can be brought together with the sample between them. The end of the rod, which is polystyrene, is softened with benzene and pressed against the sample until the benzene has evaporated and the polystyrene is hard. The rochelle salt is then dissolved away with water, and the sample is left imbedded in the polystyrene. A final Laue photograph is taken to check the sample orientation after it is affixed to the polystyrene. This was always within a degree or two of the desired position for the spheres on which data were taken.

From the description of the apparatus given above it

[1] J. H. E. Griffiths, Nature **158**, 670 (1946).
[2] C. Kittel, Phys. Rev. **71**, 270 (1947).
[3] W. A. Yager and R. M. Bozorth, Phys. Rev. **72**, 80 (1947); J. L. Snoek, Nature **160**, 60 (1947); Physica **14**, 207 (1948); A. F. Kip and R. D. Arnold, Phys. Rev. **75**, 1556 (1949); D. Polder, Phil. Mag. **40**, 99 (1949); J. M. Richardson, Phys. Rev. **75**, 1630 (1949); J. H. Van Vleck, Phys. Rev. **78**, 266 (1950).
[4] W. H. Hewitt, Jr., Phys. Rev. **73**, 1118 (1948).
[5] H. G. Beljers, Physica **14**, 629 (1949).
[6] L. R. Bickford, Jr., Phys. Rev. **78**, 449 (1950).
[7] Galt, Matthias, and Remeika, Phys. Rev. **78**, 391 (1949).

[7a] The crystal converter is driven hard by the beat oscillator signal, and under these conditions the difference frequency output is proportional to the signal from the test cavity. This proportionality has been checked experimentally in this set-up.
[8] W. L. Bond (to be published).

will be clear that we measure the *variation* in the signal transmitted through the cavity as we change the steady magnetic field H_z. All measurements are taken with the cavity tuned to resonance. From these data we find the variation in ferromagnetic resonance energy absorption with H_z in the following way. From Eqs. IV(14) and IV(16) in Slater's[9] review article on microwave electronics, when the cavity is at resonance the ratio of signal power out to signal power incident on the input window is:

$$\frac{P_{\text{out}}}{P_{\text{inc}}}=\frac{4Q_L^2}{Q_{\text{ext}_1}Q_{\text{ext}_2}}, \tag{1}$$

where Q_L is the loaded Q and Q_{ext_1} and Q_{ext_2} are the input and output Q's respectively. Here:

$$\frac{1}{Q_L}=\frac{1}{Q_{\text{ext}_1}}+\frac{1}{Q_{\text{ext}_2}}+\frac{1}{Q_a}, \tag{2}$$

where Q_a is the unloaded Q of the cavity. Q_a takes account of losses in the sample as well as in the other components of the cavity. From Eqs. (1) and (2):

$$\frac{1}{Q_a}=2\frac{V_{\text{inc}}}{V_{\text{out}}}\frac{1}{(Q_{\text{ext}_1}Q_{\text{ext}_2})^{\frac{1}{2}}}-\frac{1}{Q_{\text{ext}_1}}-\frac{1}{Q_{\text{ext}_2}}, \tag{3}$$

where $V_{\text{inc}}/V_{\text{out}}$ is the square root of $P_{\text{inc}}/P_{\text{out}}$.

Now if a reference point is established at very large H_z where the ferromagnetic resonance energy absorption is zero, Q_a at that H_z involves all the other losses in the cavity, including the dielectric losses in the sample. If a prime is used to denote quantities at the reference point Eq. (3) gives;

$$\frac{1}{Q_a}-\frac{1}{Q_a'}=2\frac{V_{\text{inc}}'}{V_{\text{out}}'}\frac{1}{(Q_{\text{ext}_1}Q_{\text{ext}_2})^{\frac{1}{2}}}\left(\frac{V_{\text{out}}'}{V_{\text{out}}}-1\right), \tag{4}$$

where we have used the fact that the incident signal is held constant during the experiment and therefore $V_{\text{inc}}'/V_{\text{inc}}=1$. Now if (1) is used to determine Q_L at the reference point and it is called Q_L', Eq. (4) becomes:

$$\frac{1}{Q_a}-\frac{1}{Q_a'}=\frac{1}{Q_L'}\left(\frac{V_{\text{out}}'}{V_{\text{out}}}-1\right). \tag{5}$$

In terms of energy dissipated per unit time, this can be written as:

$$w_m=(w_{\text{ext}_1}+w_{\text{ext}_2}+w_{\text{cav}}+w_{\text{diel}})[(V_{\text{out}}'/V_{\text{out}})-1], \tag{6}$$

where w_m is the energy dissipated due to ferromagnetic resonance, w_{ext_1} and w_{ext_2} are the energies lost through the input and output windows of the cavity, w_{cav} is the energy lost in the cavity outside the sample and w_{diel} is the *dielectric* energy loss in the sample. We assume that $(w_{\text{ext}_1}+w_{\text{ext}_2}+w_{\text{cav}}+w_{\text{diel}})$ is independent of the applied field H_z.

Two methods were used to measure the steady field H_z. One was the conventional rotating coil technique. The voltage induced in a coil rotating in a field H_z is a measure of the field. With this method we are able to obtain accuracies of ± 0.5 percent. The other method which was used for most of the readings was the measurement of the resonance frequency of protons in the field. From this and the value of the gyromagnetic ratio γ for the proton as measured by Thomas, Driscoll, and Hipple[10] the value of the field is obtained using the relation $\omega=\gamma H$. We have used a superregenerative circuit similar to that of Roberts[11] to detect the resonance. The protons were contained in a sample of polyisobutylene. The line observed is narrow enough to give an accuracy of ± 0.02 percent in the measurement, and not so sharp and intense as to cause overcoupling troubles.

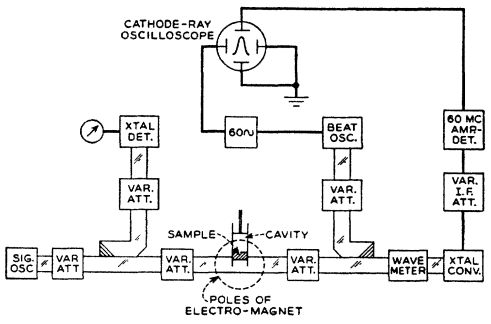

FIG. 1. Block diagram of the r-f equipment.

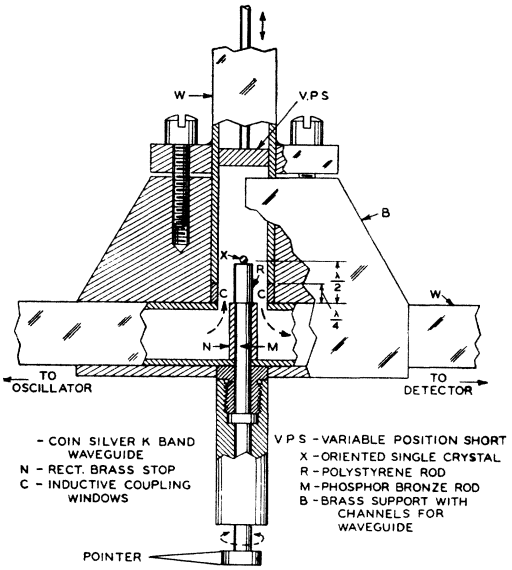

FIG. 2. Schematic diagram of the transmission cavity for magnetic resonance absorption measurements at 1.25-cm wave-length. W-coin silver K band wave guide.

[9] J. C. Slater, Rev. Mod. Phys. **18**, 441 (1946). There is a misprint in Eq. IV(14) in this reference. It should read:

$$\frac{P}{\frac{1}{2}Z_0A\bar{A}}=\frac{4Q_L^2}{Q_{\text{ext}_1}}\left(\frac{1}{Q_a}+\frac{1}{Q_{\text{ext}_2}}\right).$$

[10] Thomas, Driscoll, and Hipple, Phys. Rev. **75**, 902 (1949).

[11] A. Roberts, Rev. Sci. Inst. **18**, 845 (1947).

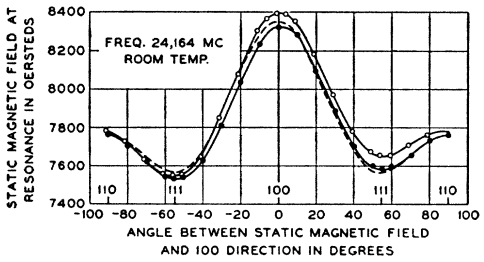

FIG. 3. Variation of H_{res} for directions in a (110) plane with the angle between the steady field and a [100] direction.

III. RESULTS

Because a crystal of nickel ferrite is magnetically anisotropic, the steady field at which maximum absorption occurs, H_{res}, is different when the steady field is applied along different crystal directions. The variation of H_{res} for directions in a (110) plane with the angle between the steady field and a [100] direction is shown in Fig. 3. Data for two spheres are shown by the two solid curves. As we shall see presently, the magnetocrystalline anisotropy constant K_1 can be determined from these data.

The width of the absorption line has required some care in its determination. Our first measurements were made on a sphere approximately 0.10 cm in diameter. The line observed is shown in the top half of Fig. 4. The essential structure of this line was the same at all crystallographic orientations. One large line and two small ones always occurred, and the separations remained quite constant. This behavior seems to be caused by electromagnetic cavity type resonances in the sample.[11a] As we go up the resonance curve $(\epsilon\mu)^{\frac{1}{2}}$ reaches a value such that a half-wave-length of electromagnetic radiation is of the order of the diameter of the sphere, and resonance occurs. We do not know enough about ϵ to check this relation by calculating $(\epsilon\mu)^{\frac{1}{2}}$; when we use smaller samples, however, a single narrow line occurs as we should expect and H_{res} is not the same as that for the maximum absorption in the larger sphere. Furthermore our best estimates of ϵ make this explanation plausible. The line obtained in a small sample at the same crystallographic orientation is plotted in the lower half of Fig. 4. It is believed to be the narrowest ferromagnetic resonance line thus far observed.

We have observed no large variation in the line width with the crystallographic orientation of the steady field. In one case the width varied from 70 oersteds when H_z was along the [100] direction in the (110) plane to 77 oersted when H_z was along the [111] direction in the (110) plane. Variations of this size occur from sample to sample, however.

We have also found that varying the position of the sample in the r-f field of the test cavity has no appreciable effect on line width. This result seems to indicate that the dielectric losses are independent of the magnetic losses, and thus to justify the assumption stated just after Eq. (4).

IV. THEORY

Using Kittel's theory for the relationship between H_{res} and crystallographic direction,[12] we can account for the data of Fig. 3 and can derive the value of the magnetocrystalline anisotropy constant K_1. According to Kittel, the general resonance condition is:

$$\omega=\gamma H_{\text{eff}}, \tag{7}$$

where γ is the gyromagnetic ratio $ge/2mc$ and g is the spectroscopic splitting factor.[13] If the z axis is taken along the steady applied field:

$$H_{\text{eff}}=\{[H_z+(N_y+N_y{}^e-N_z)M_z] \times[H_z+(N_x+N_x{}^e-N_z)M_z]\}^{\frac{1}{2}}. \tag{8}$$

N_x, N_y, N_z are the usual demagnetizing factors. $N_x{}^e$ and $N_y{}^e$ are effective demagnetizing factors, which are a convenient way of taking account of the variation in the resonance field due to the presence of magnetic anisotropy. Each of these factors takes account of one component of the torque on the magnetization due to the anisotropy. The values of $N_x{}^e$ and $N_y{}^e$ to be used in analyzing the data in Fig. 3 where the steady applied

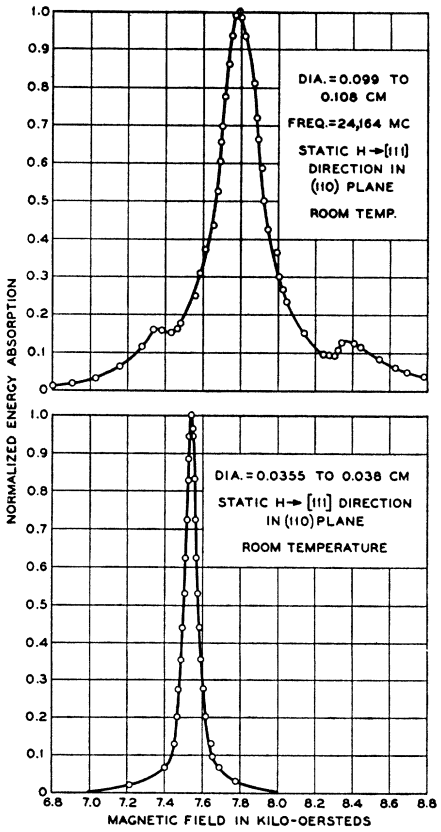

FIG. 4. Structure of the absorption line.

[11a] The authors are indebted to Dr. C. Kittel for suggesting this explanation.

[12] C. Kittel, Phys. Rev. **73**, 155 (1948).
[13] C. Kittel, Phys. Rev. **76**, 743 (1949).

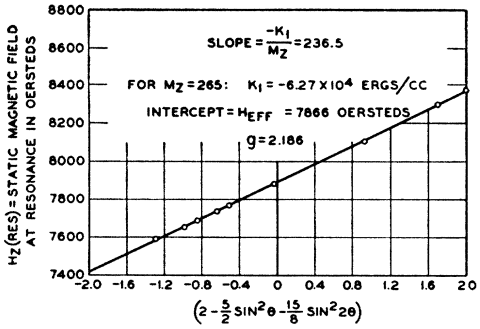

FIG. 5. Variation of the static magnetic field at resonance as determined by Eq. (12). *Note added in proof:* $g=2.186$ should read $g=2.19$.

field is always in the (110) plane have been derived by Bickford.[6] They are:

$$N_x^e=(2-\sin^2\theta-3\sin^2 2\theta)K_1/M_z^2,$$
$$N_y^e=2(1-\sin^2\theta-\tfrac{3}{8}\sin^2 2\theta)K_1/M_z^2, \quad (9)$$

where θ is the angle between the steady applied field and a [100] crystal direction.

Since we deal with spheres, $N_x=N_y=N_z$, and Eq. (8) becomes:

$$H_{\text{eff}}=[(H_z+N_y^eM_z)(H_z+N_x^eM_z)]^{\frac{1}{2}}. \quad (10)$$

It turns out from our measurements that $N_y^eM_z$ and $N_x^eM_z$ are only about five percent of H_z, so that the square roots above can be developed by the binomial theorem, and we have to a very good approximation:

$$H_{\text{eff}}=H_z+\tfrac{1}{2}(N_x^e+N_y^e)M_z, \quad (11)$$

$$H_z=H_{\text{eff}}-(2-5/2\sin^2\theta-15/8\sin^2 2\theta)K_1/M_z. \quad (12)$$

Clearly K_1/M_z and hence K_1 can be determined from the slope of a plot of H_z *vs.* the quantity in brackets in Eq. (12). The dotted line in Fig. 3 is a plot of H_z *vs.* θ as given by Eq. (12). We attribute the deviation of the data from this curve to the fact that the samples were not perfect spheres. In calculating K_1 we have eliminated this effect by using the average of four experimental values of H_z in the plot *vs.* the quantity in brackets in Eq. (12) for each value of θ; we get four values of H_z by using the data at $+$ and $-\theta$ on both spheres. The plot of these averaged values of H_z *vs.* the quantity in brackets in Eq. (12) is shown in Fig. 5. Clearly the averaging process has eliminated deviations of the sort appearing in Fig. 3. The slope of this plot can be determined to an accuracy of ± 2 percent. Using a value of 265 c.g.s units for [7,14] M_s, we find:

$$K_1=-6.27\times 10^4 \text{ ergs/cc},$$

as compared with

$$K_1=-6.2\times 10^4\pm 10 \text{ percent ergs/cc},$$

recently obtained from hysteresis loop measurements.[7]

Experimentally, we measure H_z and θ while ω and therefore H_{eff} is held constant. We may then use Eq. (12) to find H_{eff} and from this obtain g using Eq. (7). This is done most easily using the intercept of the line in Fig. 5 with the vertical axis. In this way we obtain:

$$g=2.19.$$

The shape of the resonance line can be accounted for by Kittel's equation of motion[12] plus a damping term the magnitude of which is determined by the line width. From such an equation of motion, assuming simple harmonic time dependence in the usual way, one finds the usual sort of resonance curves for the real and imaginary parts of the permeability ($\mu=\mu'-j\mu''$). The formulas are worked out here in greater detail than usual in order to compare our data with these resonance curves. Several damping terms have been suggested[2,12]; we have used one of the general form first put forward by Landau and Lifshitz.[15]

The equation of motion is:

$$d\mathbf{M}/dt=\gamma[\mathbf{M}\times\mathbf{H}]-\gamma\alpha/M(\mathbf{M}\times[\mathbf{M}\times\mathbf{H}]), \quad (13)$$

where α is a parameter, determined from the line width, which measures the magnitude of the damping force on the precessing dipole moment of the sample.

As we have said, an expression for $\chi_x=M_x/H_x$ and thus for μ' and μ'' may be derived from Eq. (13). The demagnetizing fields and the effective fields caused by magnetocrystalline anisotropy enter into these formulas, however, since they affect the effective field inside the material. There is thus no general way of plotting curves for μ' and μ'' which are characteristic of the material and independent of sample shape. The formulas for μ' and μ'' for spherical samples are given in the appendix [Eqs. (A-2)].

The parameter α is determined from the line width by means of the following relation (see appendix):

$$\alpha/(1+\alpha^2)^{\frac{1}{2}}=[(l_xl_y)^{\frac{1}{2}}/(l_x+l_y)]2\Delta H/H_{res}. \quad (14)$$

$2\Delta H$ is the width of the absorption line at points such that $\mu''=\frac{1}{2}\mu''_{res}$. Since α is small for the lines observed here, we use the approximation $(1+\alpha^2)^{\frac{1}{2}}=1$. With α determined, Eqs. (A-2) are complete, and give formulas for μ' and μ'' *vs.* H_z if ω is constant or *vs.* ω if H_z is constant. The value of α obtained with Eq. (14) from our data is approximately:

$$\alpha=4.5\times 10^{-3}.$$

The relaxation time associated with the resonance is $2Q/\omega$, where Q is $H_{res}/2\Delta H$ for the absorption line. Equation (14) then gives:

$$\tau=\frac{2}{\omega}\frac{H_{\text{res}}}{2\Delta H}=\frac{2}{\omega}\frac{(1+\alpha^2)^{\frac{1}{2}}}{\alpha}\frac{(l_xl_y)^{\frac{1}{2}}}{l_x+l_y}, \quad (15)$$

and our data yield:

$$\tau=1.5\times 10^{-9} \text{ sec}.$$

[14] C. Guillaud and M. Roux, Comptes Rendus **229**, 1133 (1949).

[15] L. Landau and E. Lifshitz, Physik. Zeits. Sowjetunion **8**, 153 (1935).

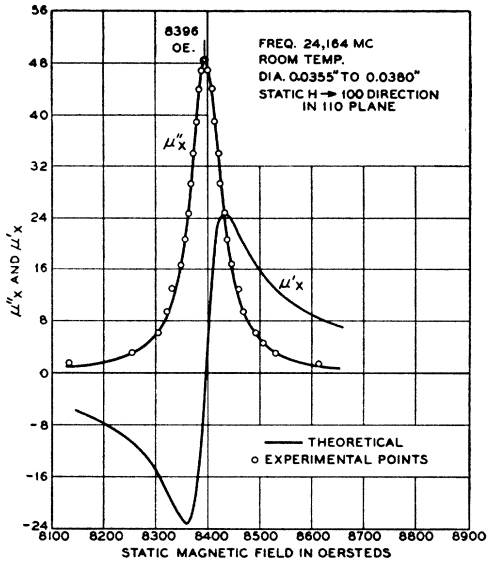

FIG. 6. Resonance curves for μ_x' and μ_x''.

The variation of μ'' with H_z as determined from experiment may be compared with Eqs. (A-2) over the whole range of variation of H as follows. The values of μ'' are first determined from the energy absorbed in the sample as given by Eq. (6). For the energy absorbed we write:

$$w_m = K\mu'', \tag{16}$$

where K is a constant proportional to the integral of H^2 over the volume of the sphere. Equation (6) then becomes:

$$\left(\frac{K}{w_{\text{ext}_1}+w_{\text{ext}_2}+w_{\text{cav}}+w_{\text{diel}}}\right)\mu''=\left(\frac{V_{\text{out}}'}{V_{\text{out}}}-1\right). \tag{17}$$

We determine $K/(w_{\text{ext}_1}+w_{\text{ext}_2}+w_{\text{cav}}+w_{\text{diel}})$ from Eq. (17) by using Eqs. (A-2) in the appendix to calculate μ'' at one point (say at maximum) and measuring $[(V_{\text{out}}'/V_{\text{out}})-1]$ at the same point. The values of μ'' can then be obtained at all other fields from Eq. (17) and compared with the curve obtained from Eqs. (A-2). Figure 6 shows a plot of the data at various points treated in this way, with the curve obtained from Eqs. (A-2) superposed. No data were taken on μ' but the theoretical curve is shown. The data fit the theoretical curve quite satisfactorily.

V. DISCUSSION

It should be noted that the g value observed here for $NiFe_2O_4$ is consistent with a very simple picture in which we attribute the whole magnetization to Ni^{++} ions as the Néel picture does for an inverse spinel of this type. The g value is then also identified with that of the Ni^{++} ions, and since the d-shell in these ions is more than half full, the g value is expected to be larger than 2.

The authors wish to express their gratitude to Dr. C. Kittel for helpful discussions of this problem, and to H. G. Hopper, W. L. Bond, and J. Andrus for technical assistance.

APPENDIX

We assume $\exp(j\omega t)$ time dependence for the x and y components of M and H, and substitute in Eq. (13) using values of the internal fields as given by:

$$\begin{aligned} H_x &= H_{x\text{app}} - N_x^e M_x, \\ H_y &= -N_y^e M_y, \\ H_z &= H_{z\text{app}}. \end{aligned} \tag{A-1}$$

Only the effective demagnetizing factors caused by anisotropy enter here. The usual ones N_x, N_y, N_z are equal for the spherical case and cancel out, so they may be dropped. We assume that $\mathbf{M}\cdot\mathbf{H}=M_zH_z$ so that the last term in Eq. (13) may be written: $\gamma\alpha(\mathbf{H}M_z-\mathbf{M}H_z)$.

The resulting equations for μ' and μ'' are:

$$\frac{\mu'-1}{4\pi}=\frac{1-\frac{\omega^2}{\gamma^2}\frac{1}{l_xl_yH_z^2(1+\alpha^2)^2}\left(1-\alpha^2\frac{l_x}{l_y}\right)}{\left[1-\frac{\omega^2}{\gamma^2}\frac{1}{l_xl_yH_z^2(1+\alpha^2)}\right]^2}\frac{M_z}{l_xH_z}, \tag{A-2}$$

$$+\frac{\alpha^2}{1+\alpha^2}\frac{(l_x+l_y)^2}{l_xl_y}\frac{\omega^2}{\gamma^2}\frac{1}{l_xl_yH_z^2(1+\alpha^2)}$$

$$\frac{\mu''}{4\pi}=\frac{\frac{\alpha}{1+\alpha^2}\frac{\omega}{\gamma}\frac{1}{l_yH_z}\left[\frac{\omega^2}{\gamma^2}\frac{1}{l_xl_yH_z^2(1+\alpha^2)}+\frac{l_y}{l_x}\right]}{\left[1-\frac{\omega^2}{\gamma^2}\frac{1}{l_xl_yH_z^2(1+\alpha^2)}\right]^2}\frac{M_z}{l_xH_z},$$

$$+\frac{\alpha^2}{1+\alpha^2}\frac{(l_x+l_y)^2}{l_xl_y}\frac{\omega^2}{\gamma^2}\frac{1}{l_xl_yH_z^2(1+\alpha^2)}$$

where

$$l_xH_z=H_z+N_x^eM_z; \quad l_yH_z=H_z+N_y^eM_z. \tag{A-3}$$

The resonance denominator makes it possible for us to calculate the field at resonance quite easily. It is:

$$H_{res}=(\omega/\gamma)[l_xl_y(1+\alpha^2)]^{-\frac{1}{2}}. \tag{A-4}$$

This checks Eq. (8) except for the factor $1/(1+\alpha^2)^{\frac{1}{2}}$ which determines the change in the resonant field caused by the damping term in the equation of motion.

If H_z is off the resonant value sufficiently to reduce μ'' to one-half of its maximum value, H_z at this point is: $H_z=H_{res}+\Delta H$. From (A-3) it is clear that at this point the two terms in the denominator are approximately equal, and therefore:

$$1-\frac{\omega^2}{\gamma^2}\frac{1}{l_xl_yH_z^2(1+\alpha^2)}=\frac{\alpha}{(1+\alpha^2)^{\frac{1}{2}}}\frac{l_x+l_y}{(l_xl_y)^{\frac{1}{2}}}\frac{1}{(l_xl_y)^{\frac{1}{2}}H_z(1+\alpha^2)^{\frac{1}{2}}}\frac{\omega}{\gamma}. \tag{A-5}$$

This can be written as:

$$\left(\frac{\gamma}{\omega}(l_xl_y)^{\frac{1}{2}}H_z(1+\alpha^2)^{\frac{1}{2}}-\frac{\omega}{\gamma}\frac{1}{(l_xl_y)^{\frac{1}{2}}H_z(1+\alpha^2)^{\frac{1}{2}}}\right)=\frac{\alpha}{(1+\alpha^2)^{\frac{1}{2}}}\frac{l_x+l_y}{(l_xl_y)^{\frac{1}{2}}}.$$

Now if (A-4) is used for ω/γ this becomes:

$$\frac{H_z}{H_{res}}-\frac{H_{res}}{H_z}=\frac{2\Delta H}{H_{res}}=\frac{\alpha}{(1+\alpha^2)^{\frac{1}{2}}}\frac{l_x+l_y}{(l_xl_y)^{\frac{1}{2}}}. \tag{A-6}$$

Equation (14) follows from Eq. (A-6) immediately.

Equations (A-2) can be simplified considerably if (A-4) is examined from a different point of view, and it is noted that the resonance frequency ω_0 associated with each field H_z is $\gamma(l_xl_y)^{\frac{1}{2}}H_z(1+\alpha^2)^{\frac{1}{2}}$. If we use this abbreviation, and the definition of τ given in Eq. (15), Eqs. (A-2) become:

$$\begin{aligned} \frac{\mu'-1'}{4\pi} &= \frac{1-(\omega^2/\omega_0^2)[1-\alpha^2(l_x/l_y)]}{(1-\omega^2/\omega_0^2)^2+(4/\omega_0^2\tau^2)}(M_z/l_xH_z), \\ \frac{\mu''}{4\pi} &= \frac{(2/\omega_0\tau)[(\omega^2/\omega_0^2)+(l_y/l_x)]l_x/(l_x+l_y)}{(1-\omega^2/\omega_0^2)^2+(4/\omega_0^2\tau^2)}(M_z/l_xH_z). \end{aligned} \tag{A-7}$$

This form reveals the resonance character of the formulas clearly.